Research Article

Received: 28 October 2014 Revised: 13 January 2015 Accepted article published: 25 February 2015 Published online in Wiley Online Library: 12 March 2015

(wileyonlinelibrary.com) DOI 10.1002/pi.4896

Preparation of new dendrimer-like star-shaped amphiphilic poly(ethylene glycol)–poly(ε-caprolactone) copolymers for biocompatible and high-efficiency curcumin delivery

Sepideh Khoee,* Alireza Kavand† and Farzaneh Hashemi Nasr†

Abstract

Novel amphiphilic star-shaped terpolymers comprised of hydrophobic poly(ε-caprolactone), pH-sensitive polyaminoester block and hydrophilic poly(ethylene glycol) (M_n = 1100, 2000 g mol^{-1}) were synthesized using symmetric pentaerythritol as the core initiator for ring-opening polymerization (ROP) reaction of ε-caprolactone functionalized with amino ester dendrimer structure at all chain ends. Subsequently, a second ROP reaction was performed by means of four-arm star-shaped poly(ε-caprolactone) macromer with eight -OH end groups as the macro-initiator followed by the attachment of a poly(ethylene glycol) block at the end of each chain via a macromolecular coupling reaction. The molecular structures were verified using Fourier transform infrared and ^{1}H NMR spectroscopies and gel permeation chromatography. The terpolymers easily formed core–shell structural nanoparticles as micelles in aqueous solution which enhanced drug solubility. The hydrodynamic diameter of these agglomerates was found to be 91–104 nm, as measured using dynamic light scattering. The hydrophobic anticancer drug curcumin was loaded effectively into the polymeric micelles. The drug-loaded nanoparticles were characterized for drug loading content, encapsulation efficiency, drug–polymer interaction and *in vitro* drug release profiles. Drug release studies showed an initial burst followed by a sustained release of the entrapped drug over a period of 7days at pH = 7.4 and 5.5. The release behaviours from the obtained drug-loaded nanoparticles indicated that the rate of drug release could be effectively controlled by pH value. Altogether, these results demonstrate that the designed nanoparticles have great potential as hydrophobic drug delivery carriers for cancer therapy.

Supporting information may be found in the online version of this article.

Keywords: star polymer; poly(ε-caprolactone); amino ester dendrimer; pH sensitive; curcumin; cancer therapy

INTRODUCTION

Interest in polymeric micelles for drug delivery applications has increased rapidly since the late 1980s.[1] These micelles are usually prepared from biocompatible amphiphilic block copolymers in aqueous media and have a series of attractive properties for drug delivery systems which can be successfully used as efficient containers for chemicals with poor solubility and/or low stability in physiological environments.[2,3]

The main factors that affect the performance of polymeric micelles for drug delivery are loading capacity, release kinetics, circulation time, bio-distribution, size and stability.[4] Nevertheless, the formation of polymeric micelles is thermodynamically favourable only above the critical micelle concentration (CMC) of the amphiphilic molecules. When the concentration drops below the CMC, the micellar structure becomes unstable and dissociates into free chains, which is one of the concerns for micelle application in *in vivo* drug delivery. When the micelles are introduced into the bloodstream, they are subjected to severe dilution and become thermodynamically unstable which leads to the burst release of entrapped drugs and may cause serious toxicity problems due to the potentially large fluctuations in drug concentrations.[5,6]

This problem can be overcome by developing multi-arm star amphiphilic block copolymers with a hydrophobic multi-arm core and large number of amphiphilic arms. Owing to their unique chemical structure and amphiphilic nature, a single multi-arm star copolymer can behave as a micelle composed of a hydrophobic core and hydrophilic shell in an aqueous solution.[7] This is in contrast to the classical multi-molecular polymeric micelles that

* *Correspondence to: Sepideh Khoee, Polymer Laboratory, Chemistry Department, School of Science, University of Tehran, PO Box 14155-6455, Tehran, Iran. E-mail: Khoee@khayam.ut.ac.ir*

† *These authors contributed equally to this work*

Polymer Laboratory, Chemistry Department, School of Science, University of Tehran, PO Box 14155-6455, Tehran, Iran

require the aggregation of multiple amphiphilic linear molecules to achieve a micellar behaviour above the CMC.[8]

Star-shaped copolymers in which hydrophobic and hydrophilic arms are connected together exhibit behaviour of unimolecular micelles,[9,10] and can possibly be appropriate for replacing linear block copolymers in applications such as drug delivery systems[11,12] and catalysis.[13] Therefore, star copolymers are expected to optimize the properties of micelles to better meet various requirements.[14] Overall, with similar molar mass and composition, star-shaped amphiphilic block copolymer-based micelles show smaller hydrodynamic radius, lower solution viscosity and significantly greater stability relative to linear polymers.[15,16] As micelle-forming materials, amphiphilic copolymers consisting of poly(ethylene glycol) (PEG) and poly(ε-caprolactone) (PCL) are attracting interest for their ability to self-assemble at low CMCs giving micelles with a solid-like core able to entrap efficiently lipophilic drugs.[17,18]

In this regard, star copolymers based on PCL and PEG with dendritic cores can be easily prepared by coupling monomethoxy-PEG (mPEG)[19,20] and its derivatives.[21,22] Wang *et al.*[23] prepared 16-arm star-shaped amphiphilic block copolymers using a second-generation polyamidoamine dendrimer as a co-initiator for the Sn(oct)$_2$-catalyzed polymerization of ε-caprolactone (CL) and then coupling of functionalized mPEG molecules to the ends of the PCL chains. In another study, Shi and co-workers synthesized core–shell structural nanoparticles based on a star-shaped amphiphilic block copolymer through ring-opening polymerization (ROP) of CL initiated by hydroxyl end-capped dendritic poly(ether amide), then coupling with mPEG via an esterification process.[24]

In the development of less toxic, better-tolerated formulations for the delivery of lipophilic anticancer drugs, polymer nanoparticle engineering approaches have provided some evidence of potential to promote tumour-specific deposition, to reduce circulating concentrations of free drug and to restrict drug distribution to noncancerous tissues due to the ability to accumulate drug at interstitial space in tumour tissue through an enhanced permeability and retention effect.[25,26]

The presence of pH-sensitive dendritic segments conjugated to the hydrophobic part in polymer micelles will enhance their functionality as carriers for cancer diagnosis and therapy.[27,28] The amphiphilic property and empty interior cavities of dendrimers could be used for physical encapsulation of various guest molecules or small particles.[29,30] In addition, as most tumour tissues are extracellularly acidic with a pH value lower than 7.4 in normal tissues, pH-responsive copolymers are more attractive for targeted drug delivery. Such a pH difference caused by the elevated level of lactic acid that is produced during tumour metabolism leads to a polymer micelle structural transition and thus encapsulated drug can be released.[31]

Curcumin is a natural, low-molecular-weight, lipophilic, yellow polyphenolic compound that is generally found in the food spice turmeric. It possesses a wide range of biological and pharmacological properties and many studies have indicated the significance of curcumin as antioxidant,[32] anti-inflammatory,[33] antimicrobial,[34] hepatoprotective,[35] anti-HIV,[36] etc. It also has been shown to have excellent anticancer activity via various molecular and cellular pathways, and has attracted much attention for its potential use as a non-toxic anticancer agent.[37] However, a problem related to curcumin is its low solubility in aqueous solution, degradation at alkaline pH, photo-degradation and poor oral bioavailability.[38] These problems can be overcome using polymeric nanoparticles without affecting its efficacy.[39,40]

In order to take advantage of these properties, our study focuses on the synthesis and characterization of multi-arm star amphiphilic sPCL-AE-*b*-(PCL)$_8$-*b*-(mPEG)$_8$ (AE, aminoester) block copolymers and the preparation of curcumin-loaded nanoparticles based on these copolymers. All the structures were characterized using Fourier transform infrared (FTIR) and ^{1}H NMR spectroscopies and gel permeation chromatography (GPC). Two different molecular weights of the hydrophilic part (mPEG) were used, and the micellar properties such as size, surface charge, CMC and morphology were investigated. Also, DSC was used to confirm the possible interaction between the polymeric matrix and the drug. Consuming different amounts of feeding drug during preparation of drug-loaded nanoparticles, the optimum drug loading and encapsulation efficiency and release level of the resulting polymeric micelles were studied. To assess the suitability of this system as a drug carrier, *in vitro* release studies were performed using curcumin as a hydrophobic model drug.

EXPERIMENTAL

Materials

Chemicals mPEG ($M_w = 1100$, 2000 g mol^{-1}), CL, pentaerythritol, stannous octoate (Sn(oct)$_2$), acryloyl chloride, 2-(ethylamino)ethanol, adipoyl chloride, 1,2-dichloromethane (DCM), diethyl ether, acetone, triethylamine, dimethylformamide (DMF), dimethylsulfoxide (DMSO) and curcumin were purchased from Merck Co. All other reagents and solvents were of analytical grade and used directly without any purification.

Polymer syntheses

Synthesis of star PCL (sPCL-(OH)$_4$)

Four-arm star-shaped PCL was synthesized by Sn(Oct)$_2$-catalysed ROP of CL using pentaerythritol as multifunctional initiator in a manner consistent with the literature.[41] Briefly, 3.88 mL of CL (35 mmol) and 0.14 g (1 mmol) of pentaerythritol were added into a three-necked round-bottom flask equipped with a magnetic stirrer and nitrogen inlet and outlet. When the temperature reached 80 °C, 0.02 g (0.05 mmol) of Sn(Oct)$_2$ was added. After that, the temperature was increased to 140 °C for 4 h with stirring. After the reaction flask was cooled to room temperature, the resulting product was dissolved in CH_2Cl_2 and then precipitated in excess cold hexane. The precipitate was filtered and washed several times with diethyl ether. The solid product was dried in a vacuum oven at ambient temperature for 24 h to obtain sPCL-(OH)$_4$ (yield 90%).

Synthesis of sPCL-(acrylate)$_4$ (sPCL-(Ac)$_4$)

Acrylation of sPCL-(OH)$_4$ was achieved by reaction of terminal hydroxyl groups with acryloyl chloride. Briefly, 4 g (1.14 mmol) of sPCL and 0.48 mL (3.4 mmol) of triethylamine were dissolved in benzene (40 mL). Acryloyl chloride (0.28 mL, 3.4 mmol) was added to the solution at 0 °C and the resulting mixture was stirred at 80 °C for 3 h. The triethylamine hydrochloride as by-product was isolated by filtration, and then the solution was precipitated into cold hexane and dried under vacuum for 24 h at room temperature (yield 70%).

Synthesis of sPCL-^{1}(OH)$_8$

The synthesis of sPCL-^{1}(OH)$_8$ was via Michael addition reaction at room temperature. In a 100 mL round-bottom flask with a magnetic stirring bar, 3 g of sPCL-(AC)$_4$ and 0.2 g of diethanolamine

(1.23 mmol) were dissolved in 10 mL of DMF. The stirred reaction was kept at room temperature for 3 days. The product was precipitated in cold water and washed sequentially with pure water to remove the unreacted diethanolamine. The precipitate was dried for 24 h in a vacuum oven at ambient temperature (yield 85%).

Synthesis of sPCL-^{1}(Ac)$_8$

The reaction procedure for acrylation of sPCL-^{1}(OH)$_8$ was the same as that for the synthesis of sPCL-^{1}(Ac)$_4$ (yield 80%).

Synthesis of sPCL-^{2}(OH)$_8$

sPCL-(OH)$_8$ was obtained by Michael addition reaction between terminal double bonds of sPCL-(Ac)$_8$ and 2-(ethylamino)ethanol for 7 days at room temperature (yield 90%).

Synthesis of sPCL-AE-b-(PCL)$_8$

The star-shaped triblock PCL–polyaminoester–PCL copolymer was synthesized by Sn(Oct)$_2$-catalyzed ROP according to the procedure described above for sPCL-(OH)$_4$ synthesis. sPCL-^{2}(OH)$_8$ and CL were used as the starting materials (yield 95%).

Preparation of sPCL-AE-b-(PCL)$_8$-b-(mPEG)$_8$

Amphiphilic sPCL-AE-*b*-(PCL)$_8$-*b*-(mPEG)$_8$ copolymers with two different mPEG (1100 and 2000 g mol^{-1}) block lengths were synthesized as follows. Measured amounts of sPCL-AE-*b*-(PCL)$_8$ and a catalytic amount of triethylamine were dissolved in a mixture of DMF–DCM (1:2) solvents (solution 1). mPEG (M_w = 1100, 2000 g mol^{-1}) was dissolved in dry DMF in a round-bottom flask and triethylamine was added as catalyst. Adipoyl chloride was added dropwise to the reaction mixture at 0 °C and the reaction system was kept at 60 °C for 24 h (solution 2). After 24 h, solution 2 was added dropwise to solution 1 and the reaction system was kept at 60 °C for 24 h. The mixture was cooled to room temperature and was poured into cold diethyl ether. The precipitated product was washed with water, and then dried under vacuum for 24 h.

Polymer characterization

The polymer structures were characterized using ^{1}H NMR (Bruker, 500 MHz) with tetramethylsilane as an internal standard and $CDCl_3$ as solvent at 25 °C and FTIR (Bruker-equinoxss) methods. ^{1}H NMR was also used to determine the number-average molecular weights of prepared products. Molecular weights and molecular weight distributions were determined using GPC (Agilent GPC 1100). The eluent was tetrahydrofuran at a flow rate of 1.0 mL min^{-1}.

Preparation of polymeric micelles

Polymeric micelles were prepared using a nanoprecipitation method. Two obtained copolymers (10 mg), sPCL-AE-*b*-(PCL)$_8$-*b*-(mPEG1)$_8$ and sPCL-AE-*b*-(PCL)$_8$-*b*-(mPEG2)$_8$, were dissolved separately in 2 mL of acetone as the organic solvent, then added dropwise to 10 mL of deionized water. The organic solvent was evaporated at room temperature under vacuum. The micelle solutions were filtered through a 0.45 μm Millipore filter to remove the aggregated particles. The mean diameter, zeta potential and polydispersity index (PDI) were measured using dynamic light scattering (DLS) at 25 °C (Nano ZS, Malvern Instruments, UK). In order to obtain nanoparticles, the micelle solutions were freeze-dried. The procedure for preparing drug-loaded nanoparticles was the same except for the measured amount of curcumin dissolved in the organic phase.

Polymeric micelle characterization

Critical micelle concentration

The CMCs of the copolymers were determined using the fluorescent probe technique with pyrene as a hydrophobic fluorescent probe as described previously.[42]

Particle size and zeta potential of micelles

Size, size distribution and zeta potential of nanoparticles were determined using a Zetasizer (Nano ZS, Malvern Instruments, UK). The mean diameter of the micelles was obtained from the number distribution curves produced by the particle analyser. For each analysis, the micelle solutions were filtered through a 0.45 μm cellulose membrane before analysis. The concentration of each sample was 1 mg mL^{-1}.

Nanoparticle morphology

The surface morphology of the nanoparticles was investigated using SEM (Hitachi S 4160). Each sample was placed on a stub and sputter-coated with gold before observation.

Drug loading, encapsulation efficiency and nanoparticle yield

The nanoparticle yield was obtained gravimetrically from

$$\text{Nanoparticle yield } (\%) = \frac{\text{Weight of nanoparticles}}{\text{Weight of feeding polymer and drug}} \times 100$$

To determine the drug loading capacity, a curcumin-loaded micellar solution was lyophilized and then dissolved in DMSO and analysed with a UV-visible spectrophotometer (Cary 100 Bio) at 425 nm, using a standard calibration curve experimentally obtained with curcumin–DMSO solutions. The drug loading content (DL) and encapsulation efficiency (EE) were calculated as follows:

$$\text{DL } (\%) = \frac{\text{Weight of drug in nanoparticles}}{\text{Weight of nanoparticles}} \times 100$$

$$\text{EE } (\%) = \frac{\text{Weight of drug in nanoparticles}}{\text{Weight of feeding drug}} \times 100$$

Two different amounts of drug (1 and 2 mg) for both polymeric micelle types (10 mg) were studied in order to investigate the maximum EE in nanoparticles.

Drug–polymer interaction studies

DSC studies of the drug and nanoparticles were carried out to investigate the physical state of the drug in this carrier and the possibility of any interaction between drug and polymer in the nanoparticles. DSC curves were recorded using a scanning calorimeter equipped with a thermal analysis data system (Pyris Diamond, PerkinElmer, USA). A small amount of nanoparticle sample or drug-loaded nanoparticle sample was placed in hermetically sealed aluminium pans and heated from 10 to 200 °C at a heating rate of 10 °C min^{-1} under nitrogen flow for both nanoparticle and drug-loaded nanoparticle samples.

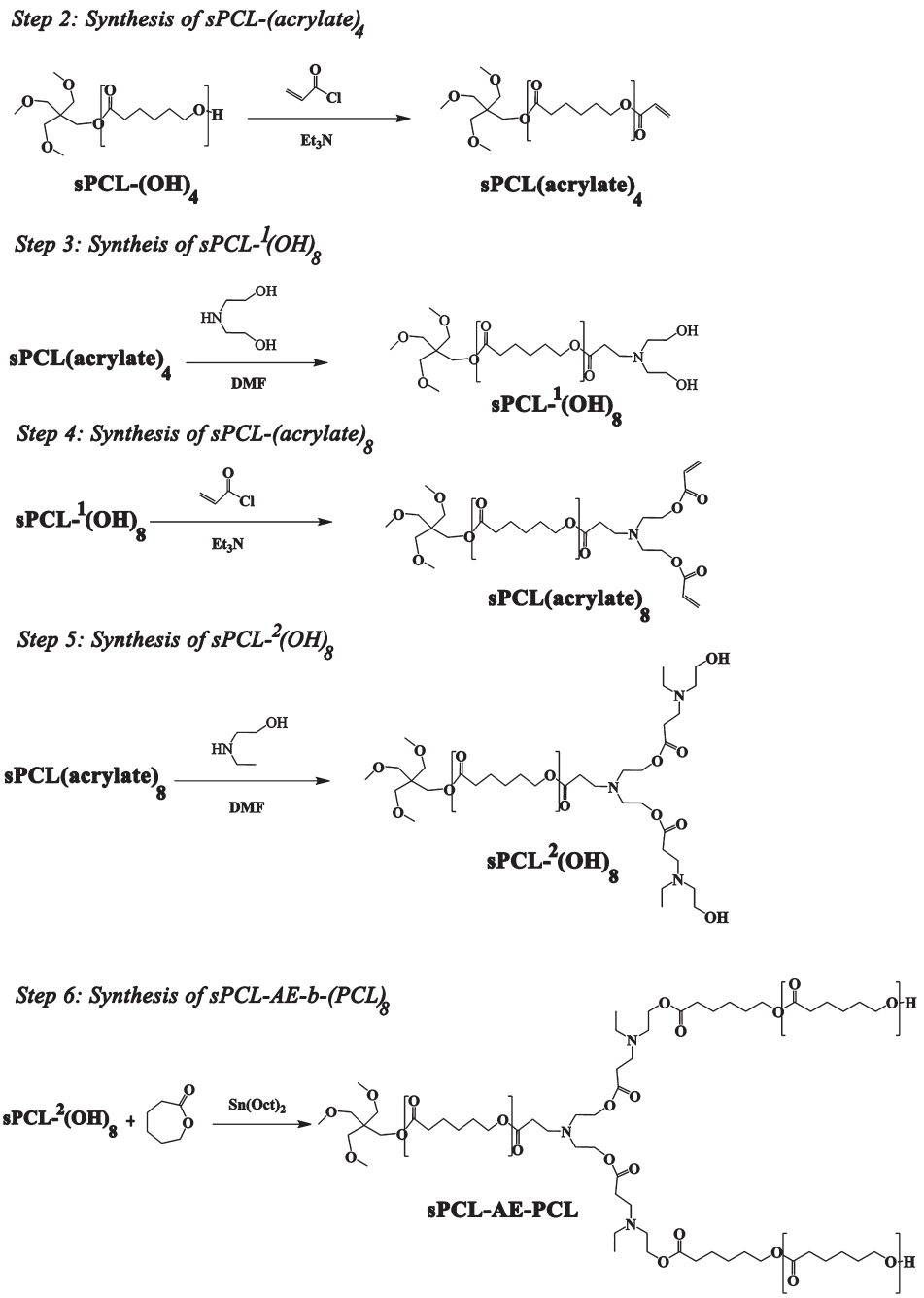

Scheme 1. Synthesis procedure steps for sPCL–AE–PCL.

In vitro release profile of curcumin from nanoparticles

In vitro drug release tests were carried out for both nanoparticle types. To study the release kinetics of curcumin from drug-loaded micelles, 0.5 mL of drug-containing micelle solution was placed in a dialysis bag (molecular weight cutoff of 12 kDa) which was incubated in 30 mL of phosphate buffer solution (pH = 7.4 and 5.8) containing Tween-80 (0.5% w/w) at 37 °C under gentle shaking. At specific times, the incubation medium was replaced with pre-warmed fresh release incubation medium. After centrifugation, the supernatant of the removed release medium was collected. The released drug was determined using UV-visible spectroscopy at a wavelength of 425 nm. This study was repeated three times, and the results were expressed as mean value ± standard deviation. The drug release can be determined from the following equation:

$$\text{Drug release } (\%) = \frac{M(t)}{M(0)} \times 100$$

where $M(0)$ and $M(t)$ represent the amount of drug loaded and amount of drug released at a time t, respectively.

RESULTS AND DISCUSSION

Synthesis and characterization of sPCL-AE-*b*-(PCL)$_8$

The synthesis procedure is shown in Scheme 1. In the first step, pentaerythritol with four hydroxyl groups is chosen as the initiator in order to produce the hydroxyl-terminated star-shaped PCL.

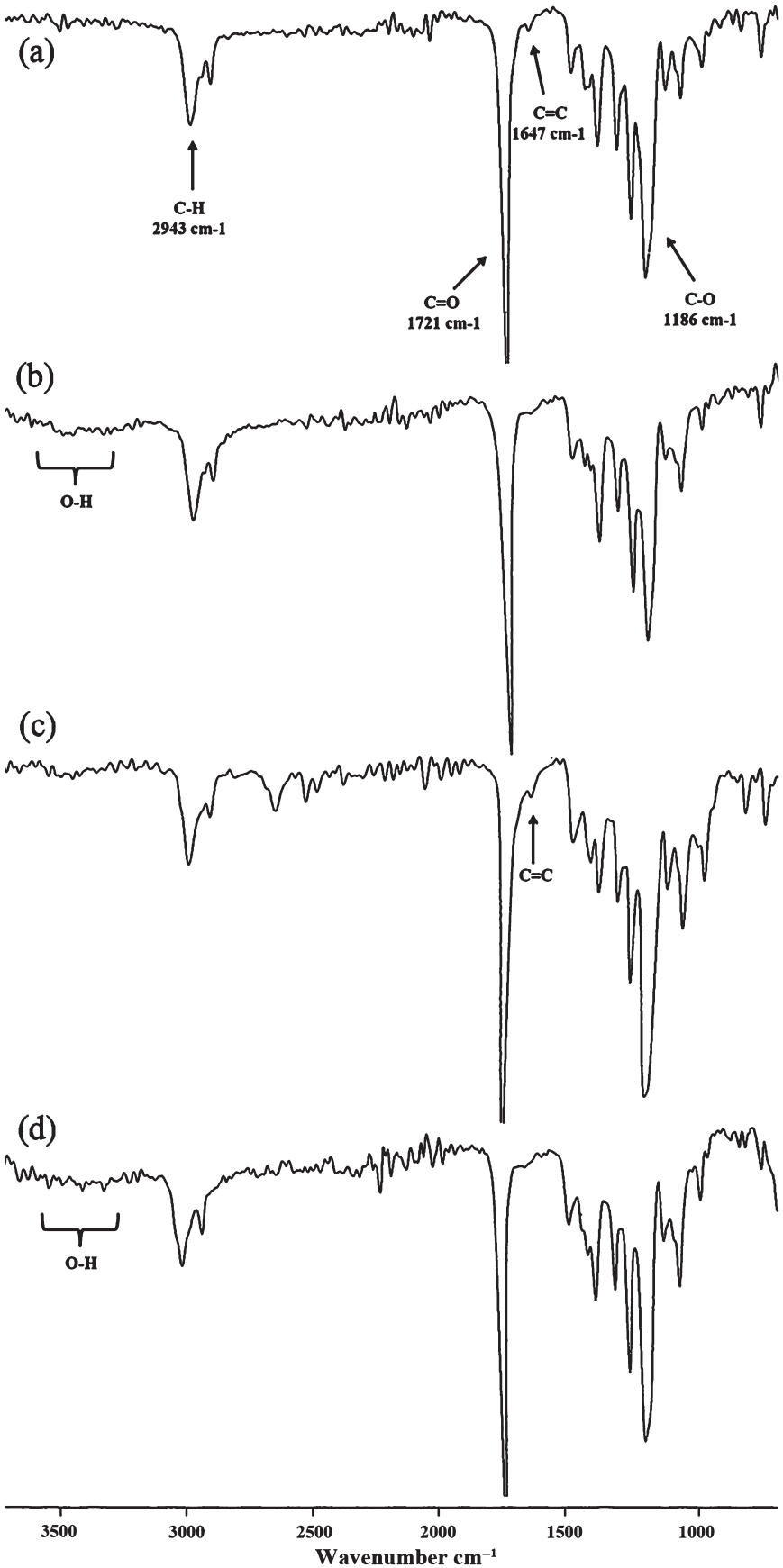

Figure 1. Representative FTIR spectra: (a) sPCL-$(Ac)_4$; (b) sPCL-$^1(OH)_8$; (c) sPCL-$(Ac)_8$; (d) sPCL-$^2(OH)_8$.

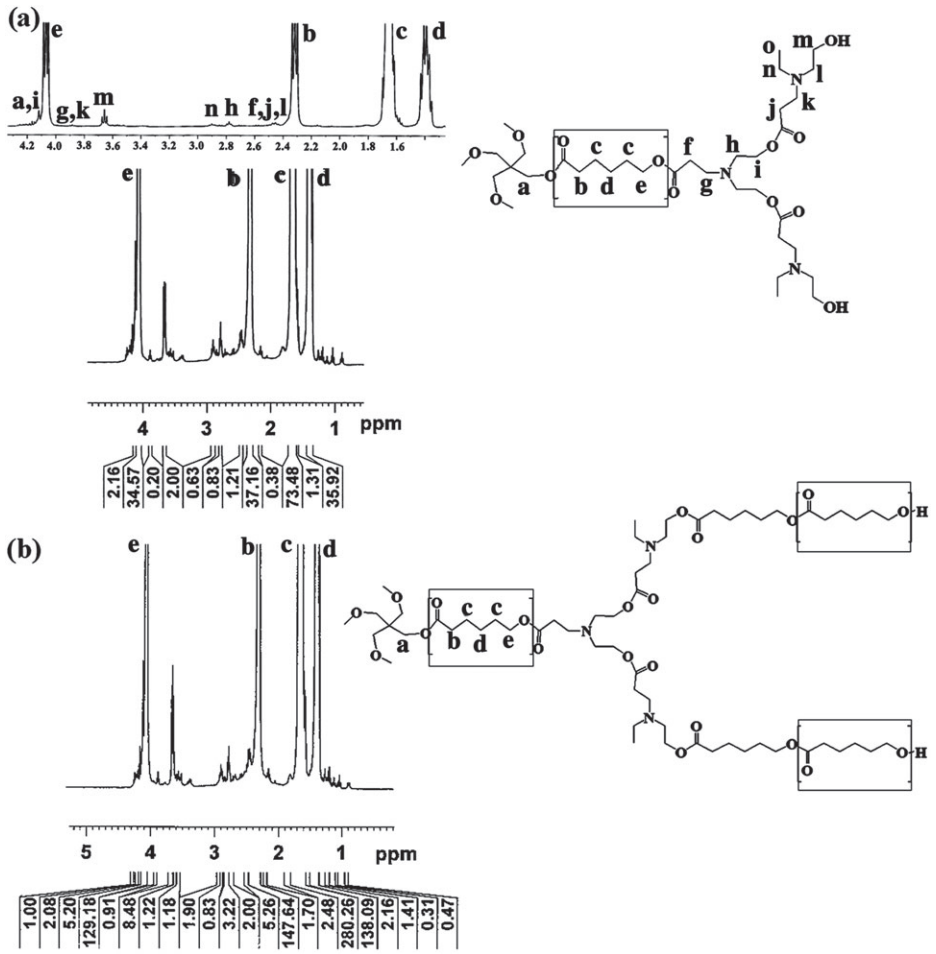

Figure 2. ^{1}H NMR spectra of (a) sPCL-^{2} $(OH)_8$ and (b) sPCL-AE-*b*-$(PCL)_8$ in $CDCl_3$.

Table 1. Molecular weights and PDIs of prepared structures

Structure	M_n[a] (g mol^{-1})	M_n[b] (g mol^{-1})	M_w[b] (g mol^{-1})	PDI[b]
sPCL-$^{2}(OH)_8$	9 355	6 100	7 500	1.22
sPCL-AE-*b*-$(PCL)_8$	13 881	9 000	15 700	1.7
sPCL-AE-*b*-$(PCL)_8$-*b* $(mPEG)_8$ (mPEG = 1100 g mol^{-1})	22 263	17 500	26 300	1.5

[a] Calculated based on ^{1}H NMR results.
[b] Obtained from GPC results.

The star-shaped PCL homopolymer is synthesized by ROP of CL at 140 °C and characterized using FTIR spectroscopy (data not shown). The spectrum shows characteristic absorption bands at 1727 and 1165 cm^{-1} for the carbonyl and C—O—C stretching of esteric groups, respectively. The absorption band at 2951 cm^{-1} is assigned to C-H stretching of initiator and PCL blocks and the wide absorption band at 2400–3500 cm^{-1} is the characteristic peak of PCL terminal OH groups.

The ^{1}H NMR spectrum of the sPCL-$(OH)_4$ is shown in Fig. S1 (supporting information). The typical signal of the methylene (a) protons of the initiator pentaerythritol is clearly detected at 4.18 ppm. The major resonance peaks (b–f) are ascribed to the protons of methylene groups in the PCL main chains.

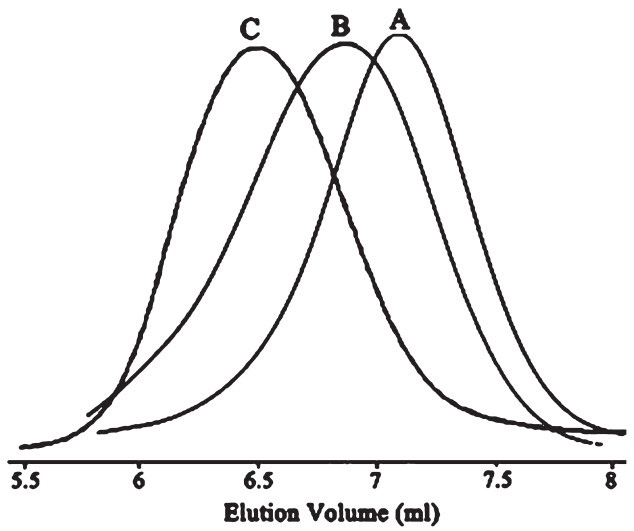

Figure 3. GPC traces: (A) sPCL-$^{2}(OH)_8$; (B) sPCL-AE-*b*-$(PCL)_8$; (C) sPCL-AE-*b*-$(PCL)_8$-*b*-$(mPEG)_8$.

The terminal hydroxyl groups of PCL chains react with acryloyl chloride in the second step to produce sPCL-$(Ac)_4$. According to Fig. 1(a), in addition to the signals already appearing in the FTIR spectrum of sPCL-$(OH)_4$, a new peak appearing at 1645 cm^{-1}

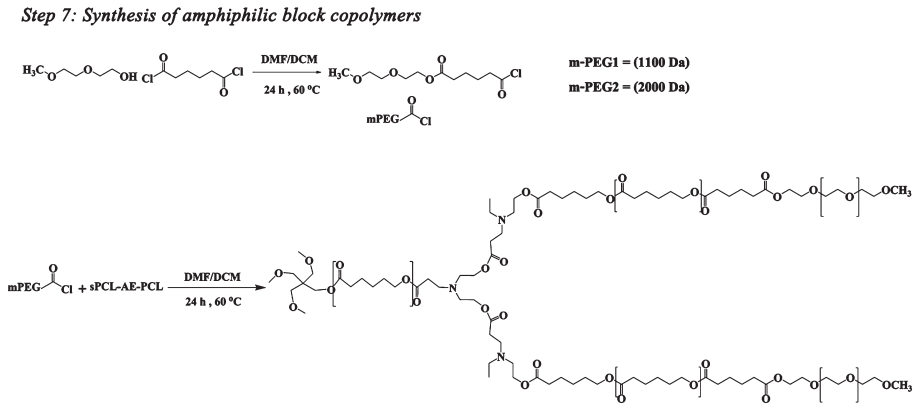

Scheme 2. Reaction pathways for the synthesis of sPCL-AE-*b*-$(PCL)_8$-*b*-$(mPEG)_8$ copolymers.

attributed to the C=C group and elimination of the absorption band at 2400–3500 cm^{-1} indicate the presence of acrylate groups.

Based on its ^1H NMR spectrum (Fig. S2), by choosing the methylene groups of pentaerythritol as the base peak ('a'), the ratio of this peak intensity to that of the protons related to acrylated groups (B) is about 1.93. This indicates that for 8 hydrogens of pentaerythritol methylene groups, there are 4 (B) hydrogens. As a result, all 4 hydroxyl groups are acrylated and the structure is mostly that of a four-arm star.

In step 3, sPCL-$^1(OH)_8$ is synthesized by Michael addition reaction between sPCL-$(Ac)_4$ and diethanolamine at room temperature. The FTIR spectrum (Fig. 1(b)) shows the disappearance of C=C peak at 1645 cm^{-1} and the appearance of a wide absorption band at 2400–3500 cm^{-1} belonging to the hydroxyl end groups. The formation of sPCL-$^1(OH)_8$ was also determined from the ^1H NMR spectrum (Fig. S2). As peaks at 5.7–6.5 ppm are no longer present, this confirms the formation of sPCL-$^1(OH)_8$.

A method similar to that for sPCL-$(Ac)_4$ preparation was used to synthesize sPCL-$(Ac)_8$ (step 4). Because of structural similarities, the FTIR spectrum as shown in Fig. 1(c) reflects the acrylation reaction with the same explanation as for step 2.

sPCL-$^2(OH)_8$ was synthesized by Michael addition of 2-(ethylamino)ethanol and the vinyl end group of sPCL-$(Ac)_8$ (Scheme 1, step 5). Noticeably, the vinylic absorption band at 1648 cm^{-1} is completely absent after the Michael reaction and a broad band corresponding to the hydroxyl end group appears at 2400–3500 cm^{-1} in the FTIR spectrum (Fig. 1(d)). For the synthesis of sPCL-$^2(OH)_8$, the reaction time was increased to 7 days in order to get a better yield and be sure of the disappearance of all acrylated groups. The ^1H NMR spectra of sPCL-$(Ac)_8$ and sPCL-$^2(OH)_8$ are similar to those of sPCL-$(Ac)_4$ and sPCL-$^1(OH)_8$.

Furthermore, in the ^1H NMR spectrum of sPCL-$^2(OH)_8$ (Fig. 2(a)), for the PCL repeat units, the triplet peaks at 4.07 and 2.32 ppm are attributed to methylene protons of —OCH_2— (e) and methylene protons adjacent the carbonyl group (b), respectively. Also, the inner methylenic protons of PCL appear as multiplets at 1.4 (d) and 1.6 (c) ppm. The peaks of the methylene protons adjacent to the nitrogen are seen at 2.9 (h), 3.65 (n) and 3.84 (k) ppm. The peaks of methylene protons adjacent to the oxygen are located at 3.65 (m) and 4.15 (i) ppm. The appearance of a new characteristic peak at 1.1 ppm (o) attributed to aminoester terminal methyl group confirms that a new branched polymer containing aminoester units has been formed.

The terminal hydroxyl groups of sPCL-$^2(OH)_8$ were used as the macroinitiator for ROP of CL in each arm in order to synthesize the sPCL-AE-*b*-$(PCL)_8$ structure. To ensure incorporation of all terminal hydroxyl groups in the second ROP and the formation of the eight-arm structure, 2-(ethylamino)ethanol was used instead of diethanolamine in step 4, in order to decrease the steric hindrance of the terminal hydroxyl groups as the macroinitiator. Actually, 2-(ethylamino)ethanol not only increases the yield of ROP but also acts as a pH-sensitive group.

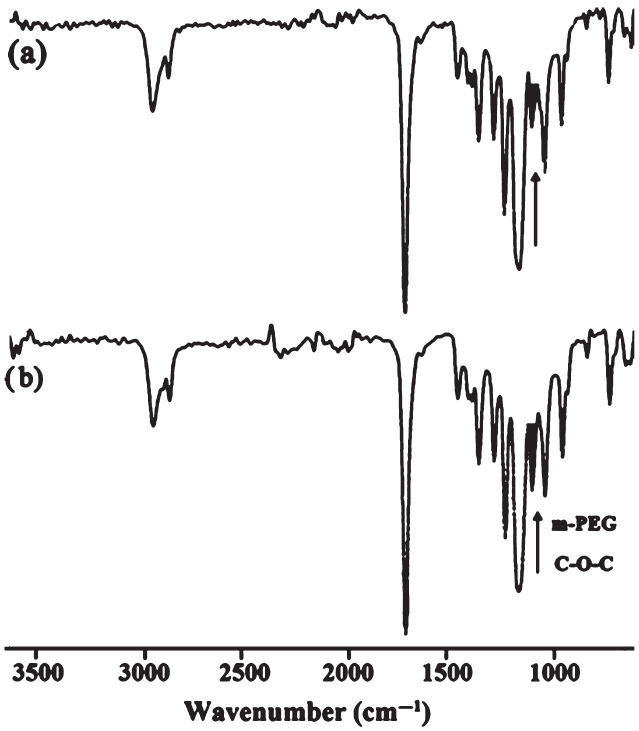

Figure 4. FTIR spectra: (a) sPCL-AE-*b*-$(PCL)_8$; (b) sPCL-AE-*b*-$(PCL)_8$-*b*-$(mPEG)_8$.

The assigned chemical structure and ^1H NMR spectrum displayed in Fig. 2(b) confirm the ROP, as the integral of signals of protons attributed to PCL block increases compared to sPCL-$^2(OH)_8$ (Fig. 2(a)). In addition, the number-average molecular weight (M_n) of sPCL-$^2(OH)_8$ and sPCL-AE-*b*-$(PCL)_8$ structures were determined using ^1H NMR which also emphasizes the increase in molecular weight. Further, their number-average and weight-average molecular weights as well as PDI were also characterized using GPC (Table 1; Fig. 3).

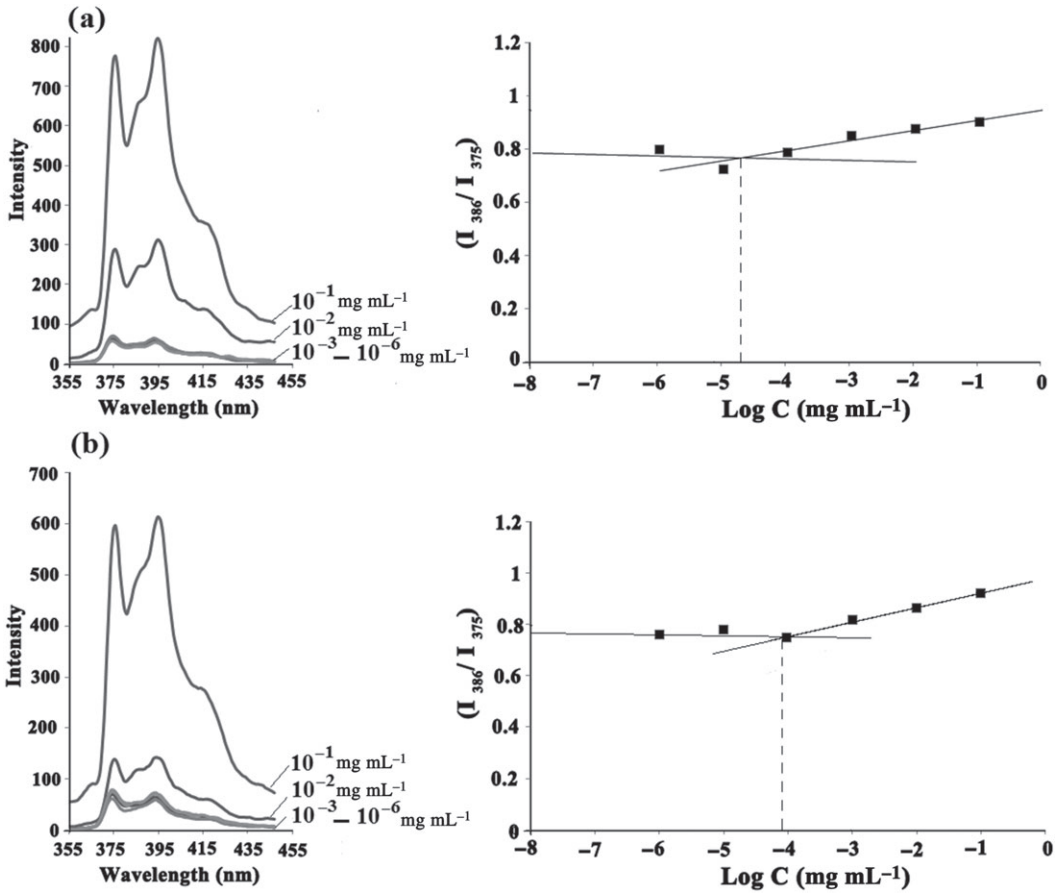

Figure 5. Fluorescence spectra of pyrene in aqueous solutions of copolymers (left) and fluorescence intensity ratios of pyrene excitation bands (I_{336}/I_{375}) as a function of concentration (right): (a) sPCL-AE-*b*-$(PCL)_8$-*b*-$(mPEG1)_8$; (b) sPCL-AE-*b*-$(PCL)_8$-*b*-$(mPEG2)_8$.

Synthesis and characterization of amphiphilic block copolymers (sPCL-AE-*b*-$(PCL)_8$-*b*-$(mPEG)_8$)

The amphiphilic copolymers were obtained via coupling reaction of mPEG using adipoyl chloride (Scheme 2). Two different molecular weights (1100 and 2000 mol g^{-1}) were selected for mPEG as the hydrophilic block.

Both prepared structures were characterized using FTIR spectroscopy. According to the spectra shown in Fig. 4, the increase of peak intensity at 1107 cm^{-1} in Fig. 4(b) compared to Fig. 4(a) proves the attachment of mPEG block to PCL chains. The band at 1107 cm^{-1} is assigned to C—O—C stretching vibrations of mPEG domains. The ^{1}H NMR data indicate the attachment of mPEG to PCL blocks (Fig. S3). Based on ^{1}H NMR integrals, the average number of mPEG (M_n = 1100 g mol^{-1}) coupled to each star polymer chain of sPCL-AE-*b*-$(PCL)_8$ is estimated to be 7.6 by calculating the integral ratio between the protons of pentaerythritol (peak 'a') and methyl protons of mPEG (peak 'm'). This means that almost all polymer chains are attached by mPEG. This illustrates that the structure of corresponding copolymer should be sPCL-AE-*b*-$(PCL)_8$-*b*-$(mPEG)_8$.

In addition to ^{1}H NMR analysis, the molecular weight of sPCL-AE-*b*-$(PCL)_8$-*b*-$(mPEG)_8$ (mPEG = 1100 g mol^{-1}) was also determined using GPC. The results are summarized in Table 1 and shown in Fig. 3.

Micellar stability and hydrodynamic size

CMC is an important characteristic of amphiphilic polymers, indicating the stability of micelles. Accordingly, the CMCs of sPCL-AE-*b*-$(PCL)_8$-*b*-$(mPEG1)_8$ and sPCL-AE-*b*-$(PCL)_8$-*b*-$(mPEG2)_8$ copolymers were estimated to investigate the core–shell structure formation using fluorescence spectroscopy with pyrene as a probe. The photophysical characteristics of pyrene as a hydrophobic molecule in the presence of polymer micelles change compared to those of pyrene molecule in water. Hence, the fluorescence intensity ratio (I_{386}/I_{375}) of pyrene *versus* logarithm of copolymer concentration is plotted to determine CMC values (Fig. 5).

Table 2. CMC, HLB, size and zeta potential of prepared copolymers

Copolymer	CMC (μg mL^{-1})	HLB	Size (nm)	Zeta potential at pH = 7.4 (mV)
sPCL-AE-*b*-$(PCL)_8$-*b*-$(mPEG1)_8$	1.6×10^{-5}	9.88	91.6 ± 2.3	−17 ± 0.12
sPCL-AE-*b*-$(PCL)_8$-*b*-$(mPEG2)_8$	7.9×10^{-5}	12.8	104.6 ± 2.7	−11 ± 0.21

Based on hydrophilicity to lipophilicity balance (HLB) of copolymers, the more hydrophilic copolymer (sPCL-AE-*b*-$(PCL)_8$-*b*-$(mPEG2)_8$) with higher HLB exhibits higher CMC than the hydrophobic one (sPCL-AE-*b*-$(PCL)_8$-*b*-$(mPEG1)_8$; Table 2). Micelles with small CMC values are expected to be more stable against dilution after injections.[43]

The size and zeta potential of both polymeric micelles were studied using DLS (Fig. 6(a)). The size distribution histogram shows

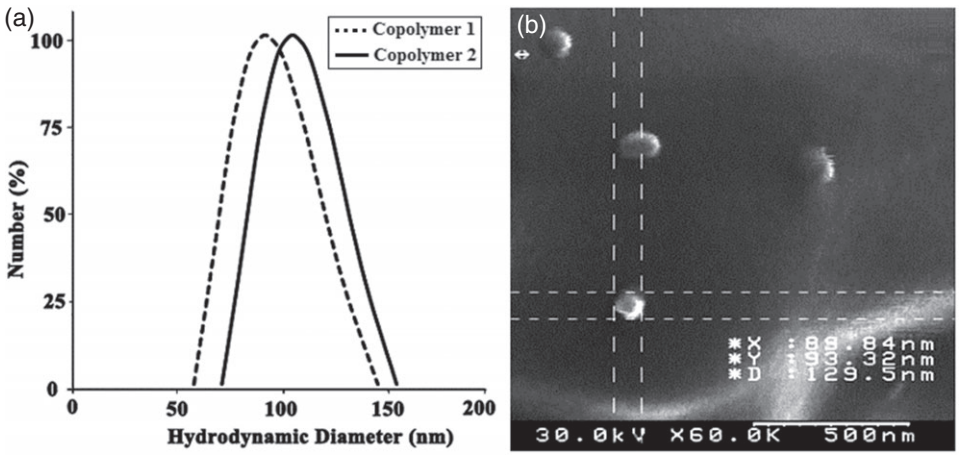

Figure 6. (a) Particle size distribution of copolymer micelles measured using DLS. (b) SEM image of sPCL-AE-*b*-$(PCL)_8$-*b*-$(mPEG1)_8$ nanoparticle.

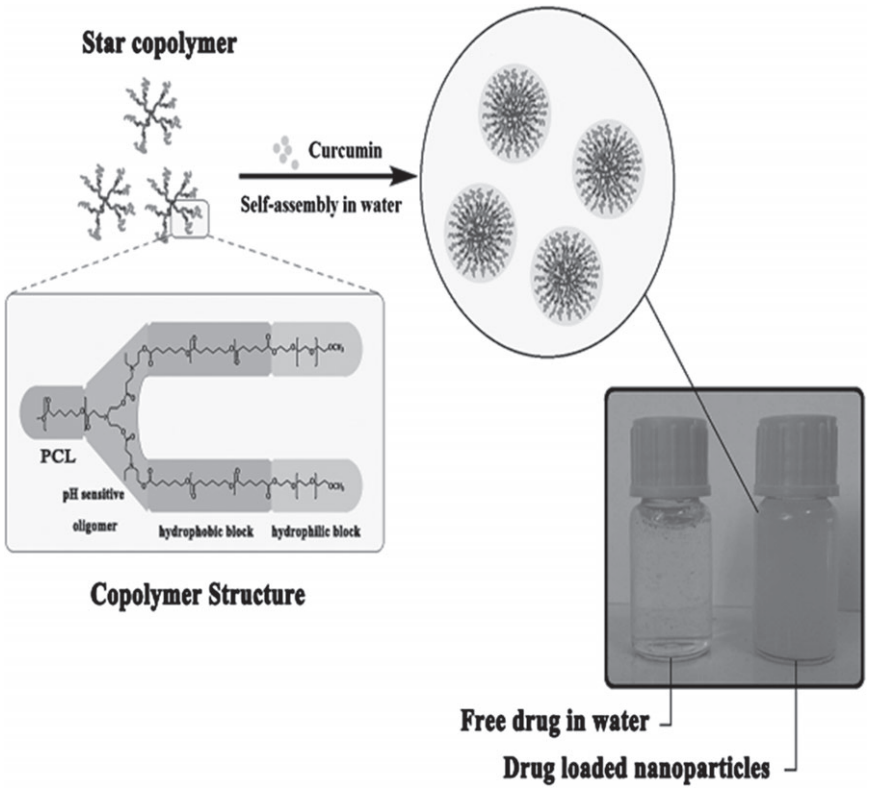

Figure 7. Copolymer structure and morphology and the comparative solubility of curcumin and curcumin-loaded nanoparticles in phosphate buffer solution (pH = 7.4).

a unimodal distribution with a particle size ranging from 91.6 to 104.6 nm with a PDI of 0.1 and negative zeta potential between −11 and −17 mV (Table 2).

Morphology studies

To further evaluate the properties of the micelles, the morphology of sPCL-AE-*b*-$(PCL)_8$-*b*-$(mPEG)_8$ micelles was also investigated using SEM (Fig. 6(b)). As shown in the SEM image, these block copolymers can aggregate into roughly spherical micelles and their average diameter is close to the result of the DLS measurement. These results indicate that the size of the prepared polymeric micelles is appropriate for tumour-targeted drug delivery.

Aqueous solubility of drug-loaded nanoparticles

The solubilities of curcumin and sPCL-AE-*b*-$(PCL)_8$-*b*-$(mPEG)_8$ nanoparticles were also determined by dissolving both curcumin and nanoparticles containing curcumin into aqueous solution and comparing with each other (Fig. 7). The star nanoparticles are completely dissolved and a clear well-dispersed liquid can be seen.

DSC analysis

Pure curcumin gives rise to a sharp melting peak at 172 °C indicating its crystalline nature.[39] As illustrated in Fig. 8(a), the bimodal melting peaks at 32.07 and 35.46 °C correspond to two different PCL segments in the star copolymer structure. The former is

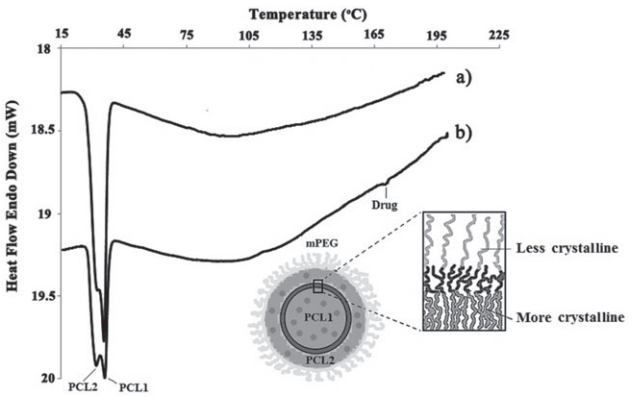

Figure 8. DSC traces: (a) sPCL-AE-*b*-$(PCL)_8$-*b*-$(mPEG1)_8$ nanoparticles; (b) curcumin-loaded nanoparticles.

attributed to PCL blocks conjugated to dendrimer blocks and PEG chains and the latter to PCL blocks connected to pentaerythritol. The DSC results confirm that the crystallization ability of PCL in copolymer composition is altered in the presence of aminoester dendrimer parts and PEG chains, suggesting the restriction and reduction in crystallinity of PCL blocks in the copolymer. According to a previous study,[44] PCL and PEG blocks are immiscible with each other, and thus they form two separated microphases as evidenced by the presence of two well-separated melting peaks in the DSC thermographs. But when the lengths of both PCL and PEG blocks are short, the separation cannot occur. Herein, the number of repeat units for the PCL block which is conjugated to dendrimer blocks and PEG chains is $n \approx 4$ in each arm. As a result, in this study the melting peak for PEG overlaps with the melting peak for PCL and does not appear separately.

It can be observed from Fig. 8(b) that nanoparticles loaded with curcumin display bimodal endothermic peaks at 31.96 and 35.86 °C and at 170 °C which represent the melting of copolymer and curcumin association in the form of micelles. This indicates that the encapsulation process does not affect the polymer structure. DSC data confirm this conclusion that there is no curcumin crystal peak in the DCS trace of the curcumin-loaded nanoparticles as the sharp peak of curcumin is absent, indicating that drug incorporated into the nanospheres is in an amorphous or disordered crystalline phase of molecular dispersion or solid solution state within the polymer matrix.

Drug loading, encapsulation efficiency and nanoparticle yield

Increase of the solubility of hydrophobic drugs and therapy efficiency enhancement are specific properties of polymeric micelles in drug release. Therefore, curcumin as a lipophilic drug for cancer therapy was loaded into the hydrophobic core of the micelles using a nanoprecipitation method.

It is reported that the hydrophobicity and length of the core-forming block have a great influence on the size and the drug loading content in the core of micelles. In fact, increasing the degree of hydrophobicity of the core-forming block improves the encapsulation efficiency and drug loading into the micelles. In addition, by increasing the corona-forming block length, the CMC will also increase, and this may result in a decrease in the aggregation number (N_{agg}) and the degree of solubilization of the hydrophobic agent into the micelles.[45] When the molecular weight of the hydrophilic segment increases from 1100 to 2000 mol g^{-1}, both DL and EE decrease. Subsequently, the effect of feeding drug amount on drug loading content was also studied. Table 3 summarizes DL, EE and nanoparticle yield of the curcumin in the micelles as a function of feeding drug/copolymer ratio. When the ratio increases from 0.1 to 0.2, DL increases while EE decreases. A drug/copolymer ratio of 0.1 was chosen for the drug release study.

Table 3. Drug loading content (DL) and encapsulation efficiency (EE) of curcumin-loaded nanoparticles with different feeding ratios

Nanoparticle	Feeding drug: copolymer ratio	DL (%)	EE (%)	Nanoparticle yield (%)
sPCL-AE-*b*-$(PCL)_8$-*b*-$(mPEG1)_8$	1:10	6.1	67	81
	2:10	6.2	37	75
sPCL-AE-*b*-$(PCL)_8$-*b*-$(mPEG2)_8$	1:10	5.5	61	71
	2:10	5.75	34.5	68

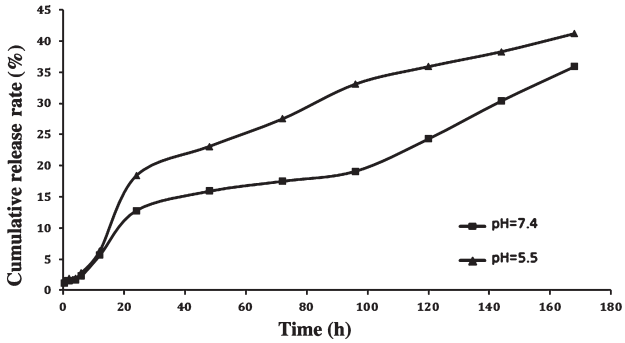

Figure 9. *In vitro* release behaviour of curcumin from sPCL-AE-*b*-$(PCL)_8$-*b*-$(mPEG1)_8$ nanoparticles at pH = 5.5 and 7.4.

In vitro drug release experiment

In order to obtain quantitative and qualitative information on drug release from sPCL-AE-*b*-$(PCL)_8$-*b*-$(mPEG)_8$ nanoparticles, the release profile was determined using an *in vitro* dialysis method. The release of curcumin was monitored in both acidic and neutral environments. As shown in Fig. 9, within 7 days, 35.9% of curcumin is released at pH = 7.4 and 41.4% at pH = 5.5. It is found that due to the presence of tertiary amine groups present in dendritic block as pH-sensitive segment, the release rate of curcumin in acidic environment increases. Noticeably, the release profile shows two steps: the initial burst step with about 10–15% of the total drug being released is observed in the first 20 h, which might be attributed to diffusion of the drug loaded on the outer surfaces of nanoparticles. The next two steps with slower release relate to the drug loaded inside the nanoparticles. The sustained curcumin release (about 40% of total curcumin) during a period of 7 days indicates the improvement of pharmacokinetics of curcumin and applicability of the designed system as a smart drug carrier with a pH-controlled releasing property for cancer therapy.

CONCLUSIONS

A novel formulation of curcumin-loaded star PCL–AE–PEG copolymer nanoparticles was designed, synthesized and characterized. These amphiphilic star block copolymers self-assemble into micelles which were characterized using DLS and SEM.

The results demonstrate that such micelles provide an excellent nano-carrier for hydrophobic drugs such as curcumin, the aqueous solubility of the drug being dramatically enhanced. Meanwhile, the encapsulated curcumin could be slowly released from the nanoparticles, which protects the drug from precipitation in physiological medium as assessed using an *in vitro* release study.

SUPPORTING INFORMATION

Supporting information may be found in the online version of this article.

REFERENCES

1 Kabanov AV, Chekhonin VP, Alakhov VY, Batrakova EV, Lebedev AS, Melik-Nubarov NS *et al.*, *FEBS Lett* **258**:343–345 (1989).
2 Choi C, Chae SY and Nah JW, *Polymer* **47**:4571–4580 (2006).
3 Lin J, Zhang S, Chen T, Lin S and Jin H, *Int J Pharm* **336**:49–57 (2007).
4 Bae Y and Kataoka K, *Adv Drug Deliv Rev* **61**:768–784 (2009).
5 Lawrence MJ, *Chem Soc Rev* **23**:417–424 (1994).
6 Ahmad Z, Shah A, Siddiq M and Kraatz HB, *RSC Adv* **4**:17028–17038 (2014).
7 Sheng Y, Nung C and Tsao H, *J Phys Chem B* **110**:21643–21650 (2006).
8 Aryal S, Prabaharan M, Pilla S and Gong S, *Int J Biol Macromol* **44**:346–352 (2009).
9 Zhou J, Wang L, Ma J, Wang J, Yu H and Xiao A, *Eur Polym J* **46**:1288–1298 (2010).
10 Pavlov GM, Knop K, Okatova OV and Schubert US, *Macromolecules* **46**:8671–8679 (2013).
11 Liu H, Miao K, Zhao G, Li C and Zhao Y, *Polym Chem* **5**:3071–3080 (2014).
12 Bahadori F, Dag A, Durmaz H, Cakir N, Onyuksel H, Tunca U *et al.*, *Polymers* **6**:214–242 (2014).
13 Pang X, Zhao L, Han W, Xin X and Lin Z, *Nat Nanotechnol* **8**:426–431 (2013).
14 Barner-kowollik C, Davis TP, Heuts JA, Stenzel M, Vana P and Whittaker M, *J Polym Sci A: Polym Chem* **41**:365–375 (2003).
15 Bílková E, Imramovsky A, Buchta V and Sedlák M, *Int J Pharm* **386**:1–5 (2010).
16 Jamal S, Rezaeia T, Nabida MR, Niknejadb H and Entezami AA, *Int J Pharm* **437**:70–79 (2012).
17 Liu JB, Zeng FQ and Allen C, *Eur J Pharm Biopharm* **65**:309–319 (2007).
18 Lapienis G, *Prog Polym Sci* **34**:852–892 (2009).
19 Nabid, MR, TabatabaeiRezaei SJ, Sedghi R, Niknejad H, Entezami AA, Oskooie HA *et al.*, *Polymer* **52**:2799–2809 (2011).
20 Bhadra D, Bhadra S, Jain S and Jain NK, *Int J Pharm* **257**:111–124 (2003).
21 Kojima Ch, Haba Y, Fukui T, Kono K and Takagishi T, *Macromolecules* **36**:2183–2186 (2003).
22 Paleos CM, Tsiourvas D, Sideratou Z and Tziveleka L, *Biomacromolecules* **5**:524–529 (2004).
23 Wang F, Bronich TK, Kabanov AV, Rauh RD and Roovers J, *Bioconj Chem* **16**:397–405 (2005).
24 Yang Z, Liu J, Huang Z and Shi W, *Eur Polym J* **43**:2298–2307 (2007).
25 Luisanna O, Marra M, Ungaro F, Zappavigna S, Maglio G, Quaglia F *et al.*, *J Control Release* **148**:255–263 (2010).
26 Chau Y, Padera RF, Dang NM and Langer R, *Int J Cancer* **118**:1519–1526 (2005).
27 Zhang X, Zhao J, Wen Y, Zhu C, Yang J and Yao F, *Carbohydr Polym* **98**:1326–1334 (2013).
28 Yuan H, Luo K, Lai Y, Pu Y, He B, Wang G *et al.*, *Mol Pharm* **7**:953–962 (2010).
29 Ciolkowski M, Palecz B, Appelhans D, Voit B, Klajnert B and Bryszewska M, *Colloids Surf B* **95**:103–108 (2012).
30 Astruc D, Boisselier E and Ornelas C, *Chem Rev* **110**:1857–1959 (2010).
31 Chen CY, Kim TH, Wu WC, Huang CM, Wei H, Mount CW *et al.*, *Biomaterials* **34**:4501–4509 (2013).
32 Pizzo P, Scapin C, Vitadello M, Florean C and Gorza L, *J Cell Mol Med* **14**:970–981 (2010).
33 Deodhar SD, Sethi R and Srimal RC, *Indian J Med Res* **71**:632–634 (1980).
34 Wang Y, Lu Z, Wu H and Lv F, *Int J Food Microbiol* **136**:71–74 (2009).
35 Kiso Y, Suzuki Y, Watanabe N, Oshima Y and Hikino H, *Planta Med* **49**:185–187 (1983).
36 Jordan WC and Drew CR, *J Natl Med Assoc* **88**:333–334 (1996).
37 Rao W, Zhang W, Poventud-Fuentes I, Wang Y, Lei Y, Agarwal P *et al.*, *Acta Biomater* **10**:831–842 (2014).
38 Shishodia S, Chaturvedi MM and Aggarwal BB, *Curr Probl Cancer* **31**:243–305 (2007).
39 Mukerjee A and Vishwanatha JK, *Anticancer Res* **29**:3867–3876 (2009).
40 Manju S and Sreenivasan K, *J Colloid Interface Sci* **359**:318–325 (2011).
41 Cheng SJ, Ding JX, Wang YC and Wang J, *Polymer* **49**:4784–4790 (2008).
42 Khoee S and Kavand A, *Eur J Med Chem* **73**:18–29 (2014).
43 Qiu LY, Wang RJ, Zheng C, Jin Y and Jin LQ, *Nanomedicine* **5**:193–208 (2010).
44 Zamani S and Khoee S, *Polymer* **53**:5723–5736 (2012).
45 Amiji M, *Nanotechnology for Cancer Therapy*. CRC Press, Boca Raton, FL (2006).

